September 25th - 28th, 2017
INTERFACES
architecture . engineering . science IASS 2017 hamburg

Proceedings of the IASS Annual Symposium 2017
"Interfaces: architecture . engineering . science"
September 25 - 28th, 2017, Hamburg, Germany
Annette Bögle, Manfred Grohmann (eds.)

Prefab, Concrete Polyhedral Frame: Materializing 3D Graphic Statics

Masoud AKBARZADEH*, Mehrad MAHNIA[a], Ramtin TAHERIAN [a], Amir Hossein Tabrizi[b]

* Polyhedral Structures Laboratory, School of Design, University of Pennsylvania, Philadelphia, US
masouda@upenn.edu

[a] The Alliance Co., Tehran, Iran
[b] AT Architects, Tehran, Iran

Abstract

This research describes the form finding and structural analysis of a prefabricated, concrete polyhedral structure designed by the use 3D graphic statics based on reciprocal polyhedral diagrams (3DGS). The form is a self-supporting, funicular polyhedral geometry with both compression and tension members Fiber reinforced, self-compacting, lightweight concrete is used to construct the members and the joints. The structure can be considered as the first built prototype designed based on the principles of the equilibrium of polyhedral frames (Rankine [22]) and the methods of 3D graphical statics as the recent development of this principle.

Keywords: Funicular polyhedral frames, concrete spatial structure, 3D graphic statics, form finding, prefabricated concrete construction, equilibrium of polyhedral frames.

1. Introduction

Either used as an analogue tool or paired with computational and optimization techniques, Geometric structural design methods, known as graphic statics (GS), are considered as one of the most powerful design techniques by many researchers and structural designers since early nineteenth century (Maxwell [15]; Rankine [21]; Culmann [10]; Cremona [9]; Anderson [6]; Van Mele et al. [24]; Beghini et al. [7]; Ohlbrock et al. [19]; Akbarzadeh et al. [2]; Lee et al. [13]). The resulting structures designed using GS methods are exemplary for structural efficiency, expressive forms, and their minimal use of materials (Fivet and Zastavni [11]; Van Mele et al. [25]). GS methods mainly fall into three following categories; 2D, 2.5D, and 3DGS methods.

1.1. 2DGS and its 2D resulting form

2DGS methods that are based on reciprocal polygonal diagrams were originally proposed by Maxwell [14] and developed by Culmann [10], Cremona [9], and many others (Wolfe [26]). Although their resulting structural forms are limited to 2D concepts, 2DGS methods were used by many eminent engineers and designers such as Guastavino, Maillart, Eiffel, Nervi, Dieste in their masterpieces (Zastavni [27]; Anderson [6]).

1.2. 2.5DGS and its 3D resulting forms

Thrust Network Analysis (TNA) (Block [8]) is a 2.5DGS method that is based on reciprocal polygonal diagrams and force density method [21]. This powerful method provides an unprecedented control in the design of 3D funicular shells. It is called 2.5DGS, for the method uses 2D polygonal reciprocal diagrams and the resulting shells are basically heightfields. Armadillo vault is a masterpiece designed using TNA (Van Mele et al. [25]).

1.3. 3DGS and its 3D resulting forms

There are various developments of 2DGS in three dimensions; the methods that are based on projective geometry and were mainly developed by Föpple [12]. These methods can be used to analyze determinate 3D truss systems, but the complexity of the projective drawings can make it quite counter-intuitive for designers. Another 3DGS

method is based on reciprocal (non-planar) polygonal diagrams proposed by Maxwell [15; 16]. There are recent developments in the use of these methods based on Combinatorial Equilibrium Modelling (CEM) as suggested by Ohlbrock et al. [19].

The third category of 3DGS that has been recently developed is based on reciprocal polyhedral diagrams originally proposed by Rankine in 1864 (Rankine [22]; Akbarzadeh et al. [4]; Akbarzadeh [1], McRobie [18]). This method is the equivalent of the existing methods of 2DGS, for the reciprocal polygonal diagrams of 2DGS are principally the planar projection of the reciprocal polyhedral diagrams. This approach provides a new horizon in the design and construction of 3D funicular forms that only their 2D examples were previously explored.

1.4. Problem statement and objectives

Although GS methods allows exploring variety of structural solutions that are in static equilibrium, it does not include material properties in the design process. Therefore, materializing the GS concepts is an important step towards the application of these methods in construction. Moreover, nothing better than a built prototype can inform designers of the structural behavior of the concept, especially if it has recently been developed.

3DGS based on reciprocal polyhedral diagrams is a promising method of form finding in three dimensions. However, like many other theories that are backed by physical experiments, this method must be attested by physical manifestations. Moreover, physical prototypes will result in better-informed GS concepts with respect to material properties.

Therefore, the main objective of this research was to build a physical prototype based on 3DGS methods to:

- apply the theory in design and construction of spatial funicular forms;
- open new directions of research in realization of such concepts by investigating material properties, fabrication techniques, and structural behavior.

2. Methodology

This section will explain the form finding and materialization of the structural concept. It starts with the development of 3DGS model and continues with the choice of material and construction techniques. An analytical model was also used to check the 3DGS equilibrium and predict the structural behavior of the system based on material properties.

2.1. Overview

The structural prototype sits on three supports placed 5.4 m from each other with the total length of 10.80 m including 129 prefabricated parts. The parts include joints and members with tensile and compressive forces (Figs. 1, 2). All parts are constructed from Glass Fiber Reinforced Concrete except the steel supports and the connectors of the tensile members. The total weight of the structure is 5480.64 kg where the heaviest joint and member weigh 103.8 kg and 126.8 kg respectively (Table 1).

2.2. Structural form finding

The main objective in the form finding process was to find an efficient spatial structural form with both compressive and tensile members using 3DGS methods. The reciprocal relationship between the form and its force diagram in 3DGS allows for explicit control over the magnitude and the type of internal as well as external forces in a structural form. To produce concepts with both compressive and tensile members, a designer can geometrically manipulate the equilibrium of external forces, referred to Global Force Polyhedron (GFP), to explore compression and tension systems without changing the topology of the form diagram (Akbarzadeh [1]).

Figure 1: A photograph of the built structure in Sa'dabad Complex, Tehran, Iran.

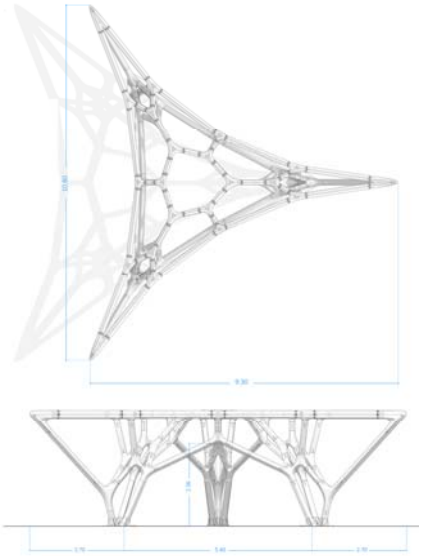

Figure 2: Plan, elevation and axonometric view of the built structure.

Table 1: General specifications of the structure.

Structure's specifications	**# of parts**	**Volume** $[m^3]$	**Weight** $[kg]$
Tensile members	30	1.003	1765.28
Compressive members	54	0.911	1603.36
Joints	45	1.2	2112
Heaviest joint	–	0.059	103.84
Heaviest member	–	0.0721	126.896
Total	129	3.114	5480.64

Table 2: Mechanical properties of the construction materials of the

Material	**Mechanical properties**		**unit**
(GFRC) Concrete	Max Compressive Strength (7-day)	15.4	$[MPa]$
	Max Compressive Strength (28-day)	23.3	$[MPa]$
	Max Tensile Strength	2	$[MPa]$
	Density	1760	$[kg.m^{-3}]$
	Young's Modulus (E)*	22.6	$[GPa]$
	Shear Modulus (G)	8	$[GPa]$
Steel	Plates $ST12$ $(t = 4mm)$ (f_y)	270	$[MPa]$
	Rebars $A2$ $(d = 12mm)$ (f_y)	380	$[MPa]$

$^* E = 4700 * \sqrt{f'_c}$; f'_c : *28-day compressive strength*

2.2.1. Manipulating GFP

For a given geometry of a form diagram, changing the direction of the external forces in GFP alters the magnitude and the type of internal forces in the form. As a rule of thumb, in a force diagram, if all Nodal Force Polyhedrons (NFP) are contained within the volume of a GFP, there exists a form configuration with compression or tension-only members. However, if the volume of GFP does not contain all NFPs, the form diagram will have members with both compressive and tensile forces (Akbarzadeh [1], Lee et al. [14]).

Besides, if GFP is geometrically indeterminate, changing the magnitude of an applied force without changing its direction can also result in a structural form with both compression and tension members. Figure 3 illustrates a compression-only structural form and its indeterminate GFP in 3D where excluding the force $\mathbf{f}_p$ from the boundary condition results in a structural form with both compression and tension forces.

Note that the force diagram will transform from convex–only polyhedral cells for a compression-only configuration of forces to a diagram with complex (self–intersecting) polyhedral cells for a compression-and-tension combined forces. Therefore, the computational framework suggested by Akbarzadeh et al. [4] can be used to explore topologically-different compression-only structural forms from convex polyhedral cells that later can be translated into forms with combined forces by changing their GFP.

2.2.2. Compression-only form finding by aggregating GFP

Aggregating convex polyhedral cells can be used as a technique in finding compression-only structural solutions. The aggregated polyhedral cells are the NFPs for a GFP that encloses them all. Similarly, GFPs can be aggregated to construct a bigger GFP and structure if their attaching faces are identical with opposite normal directions. Figure 4a illustrates three identical GFPs of Fig. 4 attaching to each other from faces corresponding to their reaction forces labeled as $\mathbf{r}_B$ and $\mathbf{r}_{C'}$. Once aggregated, the shared face is removed from the resulting force diagram and nodes B and C, will be collapsed to a single vertex in the structural form (Fig. 4b). By removing the lateral forces ($\mathbf{f}_k$, $\mathbf{f}_j$, etc.) from the boundary condition and the force diagram, the resulting funicular form will have both compression and tension members (Fig. 4c).

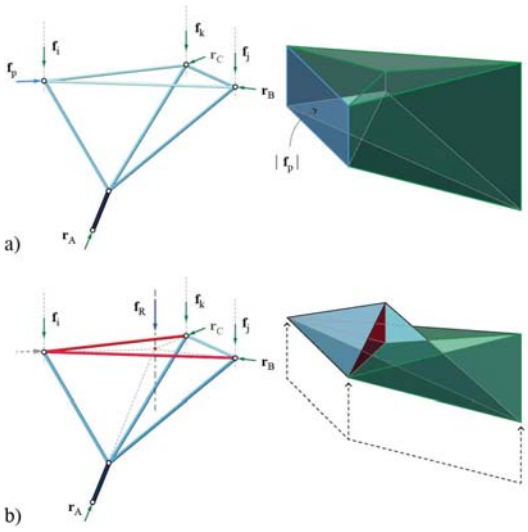

Figure 3: a) Compression-only form and force diagrams in 3DGS with indeterminate GFP; and b) form and force diagrams with mixed compression and tension forces as a result of subtracting the force $\mathbf{f}_p$.

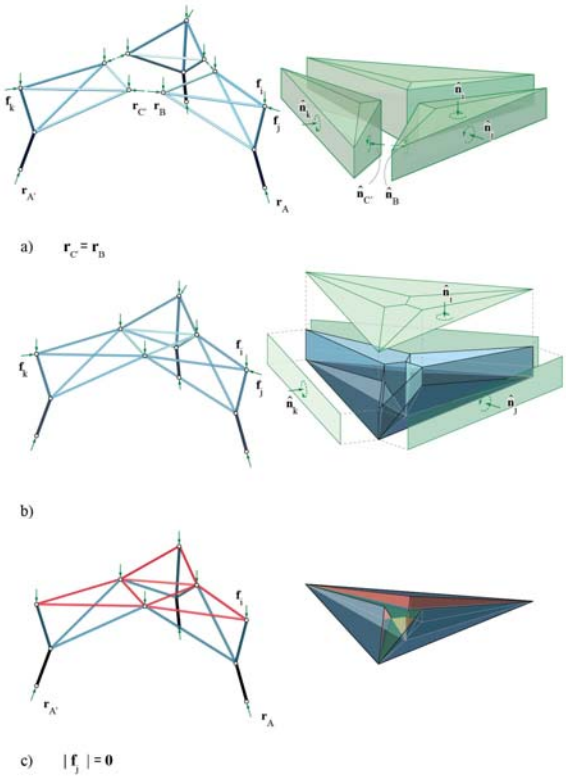

Figure 4: a) Aggregation of three GFPs and their corresponding forms; b) the resulting force diagram after removal of the shared face and its corresponding form; and c) removing lateral forces to obtain compression and tension combined form and force diagrams.

2.3. Constrained 3DGS model

In order to precisely control the location of supports and the magnitudes of the lateral loads, a constrained form and force diagrams should be constructed using procedural 3DGS in a parametric environment (Akbarzadeh [1]).

2.3.1. Establishing GFP

The first step in constructing a constrained parametric model is to establish global equilibrium (Akbarzadeh et al. [3]); we can substitute all vertically applied forces with a single resultant force $\mathbf{f}_R$ and find the direction of the reaction forces in the supports by choosing a point on the line of action of $\mathbf{f}_R$ (Fig. 5a).

Note that the laterally applied forces $\mathbf{f}_h$ also intersect the line of action of $\mathbf{f}_R$. Moreover, each force $\mathbf{f}_h$ is coplanar with a reaction force and $\mathbf{f}_R$, due to planarity constraints of the reciprocal polyhedral diagrams (Akbarzadeh et al. [3]). If the magnitude 1kN is assigned to $\mathbf{f}_R$, we will have the normalized values for reaction forces (0.35 kN) and internal forces with respect to the total applied force $\mathbf{f}_R$. Since the global force polyhedron is geometrically indeterminate, the magnitude of the lateral forces can be changed to make compression-and-tension combined systems.

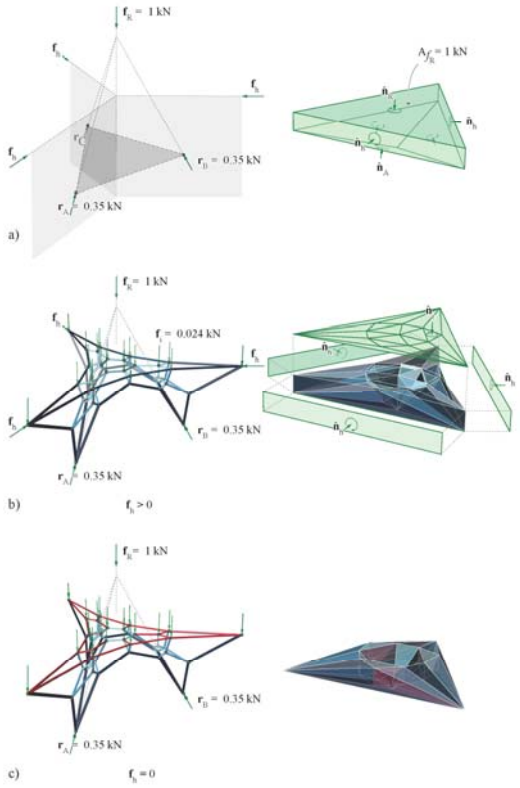

Figure 5: Construction of the constrained 3DGS model; a) establishing the global equilibrium and the equilibrium of external forces; b) subdividing the global force polyhedron and extracting the constrained, compression-only structure; and c) removing the lateral forces in the boundary condition to get the compression-and-tension-combined structural form.

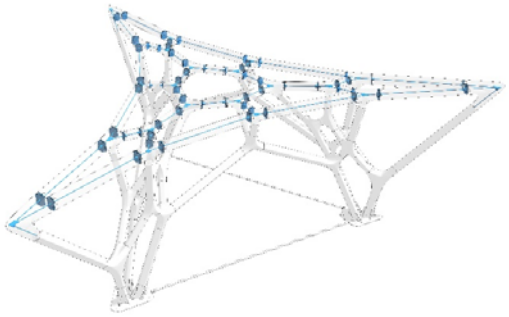

Figure 6: The rebars are embedded in the cross section of the tensile members, connected to steel plates at the end of each member.

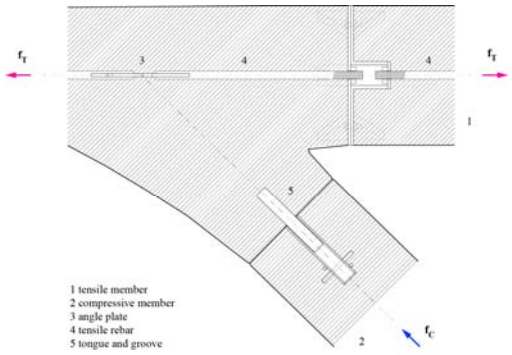

Figure 7: A section illustrating the connection details of a joint and its adjacent tensile and compressive members.

2.3.2. Subdividing GFP

Once the GFP is established, its internal space can be subdivided into convex polyhedral cells to construct a topology of a compression-only structural form (Akbarzadeh et al. [5]). The result is a spatial frame of Fig. 5b constrained to the given boundary conditions.

2.3.3. Changing boundary conditions

The magnitude of the laterally applied loads $\mathbf{f}_h$ can be achieved by reducing the area of their corresponding face to zero in the force diagram. This will result in a structural concept that has tensile forces on the top chord supported by compression-only members on the lower parts of the structure (Fig. 5c).

2.4. Materializing the concept

As soon as the static equilibrium of the structural concept is guaranteed and the 3DGS edge- vertex model is extracted, the members and joints of the structure need to be designed and sized according to the physical properties of the chosen construction materials and applied loads.

2.4.1. GFRC concrete

Glass fiber reinforced concrete (GFRC) in prefabricated elements was chosen as the construction material and method for the project. The main intention was to extend the use of concrete in design and fabrication of discrete spatial systems as oppose to its conventional use as a cast-in-place material for shells and continuous surface structures. Table 2 summarizes the mechanical properties of the used concrete in this project. To reduce the self-weight of the concrete, perlite, pumice aggregate, silica fume and chopped glass fibers were used as the main ingredients.

2.4.2. Sizing the members

The members of the structure were designed and sized according to the following criteria:

- maximum allowable stress in each member based on the applied loads;
- minimum dimensions required for concrete construction feasibility;
- and, the maximum weight of each member for prefab construction.

The magnitude of the internal forces in the members of the structure can be extracted from the areas of their corresponding faces in the 3DGS model. The values are relative to the magnitude of the resultant applied force $\mathbf{f}_R$. The cross section radii of the members were chosen to range from 7.5 to 10 cm based on the lowest and highest internal forces and construction feasibility.

To preserve the design consistency, the tensile members on the top chord of the structure were also constructed out of concrete. To improve their tensile capacity a single steel rebar (d = 12mm) was embedded in their cross section to carry tensile forces between the joints (Fig. 6).

2.4.3. Detail development

To preserve the clarity of the structural system, connection details were carefully developed to avoid any unnecessary element. In this regard, the compressive and tensile members were treated differently; the members carrying compressive forces include a hollow metal tube at their both ends to be connected to their adjacent joints which will have a pipe with a smaller diameter (Fig. 7). These simple male-and-female pipe connections can control the precision of the assembly and provide relative stability for the system during assembly obviating the need to use complicated falsework/formwork (Fig. 8). There is a dry connection between the compressive members and the joints and the axial compressive force in the members will keep them in place after completion.

The tensile members, on the contrary, include a rebar that is connected to two steel plates (t = 4mm) at both ends. These plates transfer the tensile force to the plate of the adjacent joint. In the adjacent joint the tensile force is transferred via a rebar to a custom-cut plate at the center receiving all the tensile forces from adjacent members in precise angles to keep the static equilibrium of the node and the structure (Fig. 9).

Figure 8: A photograph during the assembly process showing a compressive joint (bottom) and a tensile joint (top), dry connections between the compressive joints and members, and the conventional scaffolding system to support the unfinished structure.

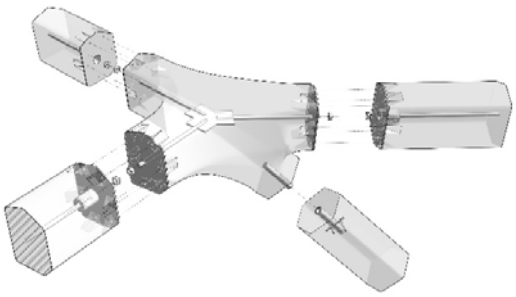

Figure 9: Exploded axon of a joint with three adjacent tensile members (top) and a compressive member (bottom) revealing the tensile rebars, connecting plates, and the custom cut plate to control the angles of the rebars within the joint.

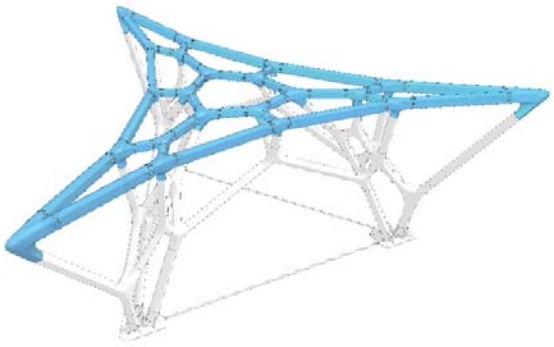

Figure 10: The weight of the tensile members is considered as the applied load $\mathbf{f}_W$ for the built structure.

2.5. 3DGS design loads vs self–weight

The 3DGS model guarantees static equilibrium of forces under the applied loads at the top vertices of the structure, but the finished structure will not have external applied loads, and it has to support its self-weight. Moreover, 3DGS model does not consider self–weight of the system. Nevertheless, constructing tensile members in the top chord of the structure can improve the structural performance of the system. Although tensile members can significantly increase the self–weight of the system, their weight (1765 kg) can also be considered as external applied loads for the structure and keep the system in equilibrium i.e. $\mathbf{f}_W$ = 17.65 kN (Fig. 10).

In this case, we need to check whether the 3DGS design force fi per vertex of the top chord is equal to the tributary load fiw resulting from the weight of the tensile members connected to the same vertex in the structure.

The tributary load values per vertex of the top chord is calculated and normalized with respect to the total weight of the tensile members (1765 kg). These values are then compared with the 3DGS design load per vertex (the area of the corresponding face in the force diagram), and it is concluded that for this specific geometry and the chosen member sizes, the discrepancies between the 3DGS design loads and the tributary loads per vertex are negligible (Fig. 11).

Table 3: Some of the analysis results and its comparison with maximum tensile and compressive stress of the used concrete.

Self–weight analysis results	**Maximum values**	**unit**
Displacement	0.025	$[cm]$
Axial tensile stress	0.078	$[kN/cm2]$
Axial compressive stress	0.0039	$[kN/cm2]$
Tensile stress for concrete	0.2	$[kN/cm2]$
Compressive stress for concrete	2.3	$[kN/cm2]$

2.6. Analytical model vs 3DGS model

To check the credibility of the 3DGS model and also to investigate other important structural behavior of the system, an analytical model was developed and analyzed using Karamba plugin (Preisinger [20]) for Rhinoceros (McNeel [17]). The analytical model with the same cross sections and boundary condition was analyzed to find:

- the magnitude of the axial forces in the internal members as a result of the application of the 3DGS design loads;
- and the maximum displacement of the nodes based on self–weight of the structure.

2.6.1. Axial forces in the structure based on 3DGS loads

To check the results of the 3DGS equilibrium and the internal forces of the structure, the model were subjected the 3DGS design loads. As is shown in Fig. 12a, the magnitude of the internal forces in the analytical model subjected to the 3DGS design loads precisely matches the values of the faces of the force diagram in 3DGS.

If the construction material has a really high elastic modulus, its behavior will be very close to what is expected based on 3DGS model. Given the size of the members and the mechanical properties of the used concrete, the resulting structure was relatively stiff and therefore, the analysis results match the static equilibrium of forces in the 3DGS model quite well.

2.6.2. Displacement based on self-weight

Since the 3DGS model does not consider the self-weight of the members, the concept should be analyzed under its own weight (Fig. 12b). Table 3 summarizes some of the analysis results based on self-weight of the structure. The results show that the maximum displacement is 0.025 cm which is smaller than (L/360 = 270/360 = 0.75 cm).

3. Conclusions and Discussions

The paper described the form finding and materialization process of the first built prototype designed by the use 3DGS methods. Various GS design techniques such as compression-only form finding, aggregating GFPs, constrained modeling, and modifying the boundary conditions were used to derive a compression-and-tension combined, funicular polyhedral system.

GFRC was used as the primary construction material and the members were sized according to their internal forces derived from the 3DGS model (from 15 to 25 cm). The tensile members were designed with a steel rebar embedded in their cross section. Since 3DGS model does not account for the self-weight of the members and the final structure will only be subjected to its self-weight, the weight of the tensile members was considered as the applied loads for the structure.

Accordingly, the magnitude of the tributary loads from the tensile members per vertex on the top chord were compared with the magnitude of the 3DGS design force and showed negligible differences. This little difference might be related to the geometry of the form with specific member length and sizes. These differences might not be negligible for large scale structures and therefore, certain optimization techniques are required to match the 3DGS design loads with the tributary area of the vertices. Another future research direction is to incorporate the self-weigh of the members in the 3DGS model in the design process.

The analysis result of the FEM model subjected to 3DGS external forces matched the equilibrium results of the 3DGS model and confirmed the validity of this technique. However, further research is required to understand the geometric and mechanical parameters that can affect the results significantly for large scale structures.

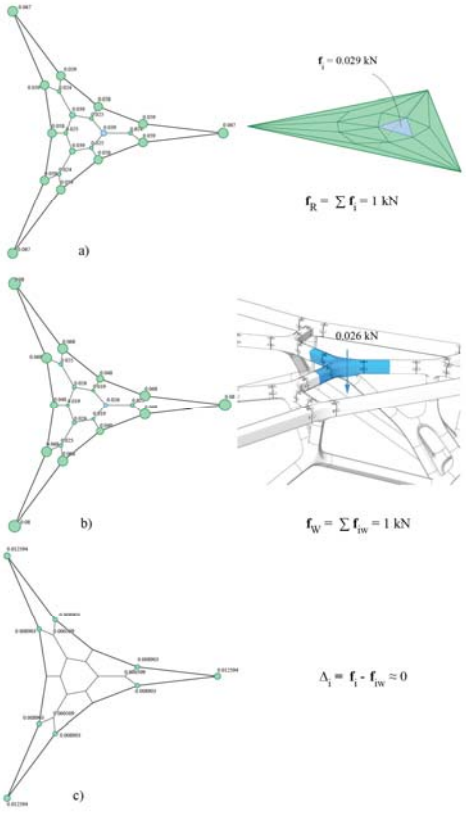

Figure 11: The deviation from the 3DGS design loads and the weight of the tensile members as the externally applied loads of the structure; a) the normalized value of forces per vertex of the structure corresponding to the areas of the faces of GFP; b) the normalized values of the tributary loads per vertex based on the weight of the tensile members; and c) the negligible differences between the 3DGS design loads and the tributary loads per vertex.

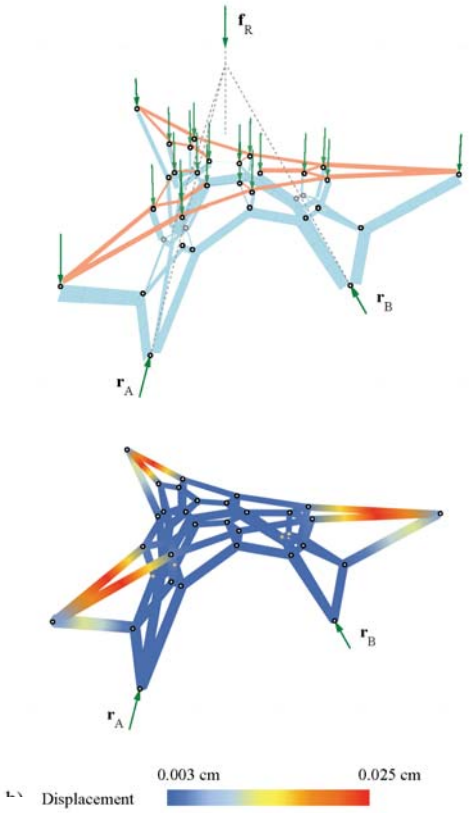

Figure 12: The magnitude of the axial internal forces under the 3DGS applied forces (top); displacement of the nodes based on the self–weight of the structure (bottom).

Acknowledgements

The work presented in this paper was a result of a workshop in 3D graphic statics with 31 participants in collaboration with various material and machining service providers. The authors of the paper would like to thank all the students who worked on the project, people whose hard work and endeavor played a significant role during both design and fabrication processes: Nematollah Safari, Alireza Bayramvand, Parham Gholizadeh, Soroush Garivani, Fatemeh Salehi Amiri, Seyed Ali Mirzadeh, Nastaran Saeidi, Niloofar Imani, Pooria Gachpazan, Maryam Shahabi, Sobhan Sarabi, Armin Shayanpour, Yasamin Samaee, Kimiya Safakhah, Anahid Attaran, Banafsheh Tavassoli, Sepehr Farzaneh, Ayeh Fotovat, Maryam MollaAsadollah, Shahryar Abad, Neshat Mirhadizadi, Mohammad Hossein Karimi, Mohammad Ebrahimi, Pedram Karimi, Mobin Moussavi, Mehrzad

Esmaeili Charkhab, Sahar Barzani, Atiyeh Sadat Fakhr Hosseini, NiloufarNamdar, Setareh Houshmand, Ehsan Heydarizadi. We are also thankful to Contemporary Architects Association for organizing the workshop and Sa'adabad Complex officials for hosting the final prototype.

The fabrication process was conducted in collaboration with the following companies: CODON Interactive Media: 3D printing; Horon Co.: CNC milling; ParsFoamCut: wire cutting of polystyrene foam blocks; Fateh Workshop: laser cutting and CNC bending services of metal sheets; and, Vandidad Sepehr Co.: light weight concrete mixture and material of the project.

The project was partially funded by Cultural Heritage, Handicrafts and Tourism Organization of Iran, Kheiri Co, Omid Amini and Partners, and Sizan Co. In addition, the authors would like to express their gratitude towards Alireza Behzadi, Sina Ahmadi, Kristjan Plagborg Nielsen, Abbass Naseri, Nima Sadeghinejad, Davoud Mohammad Hassan, Amirali Zinati, Paniz Farrokhsiar, Mehdi MollaAsadollah, Ahmad and Gholam for their individual contribution to make this work possible.

References

[1] Akbarzadeh M.*, 3D Graphic Statics Using Reciprocal Polyhedral Diagrams*. PhD thesis, ETH Zurich, Zurich, Switzerland, 2016.

[2] Akbarzadeh M., Van Mele T., and Block P., Compression-only form finding through finite subdivision of the external force polygon. *In Proceedings of the IASS-SLTE 2014 Symposium*, 2014, Brasilia, Brazil.

[3] Akbarzadeh M., Van Mele T., and Block P., 3D Graphic Statics: Geometric construction of global equilibrium. *In Proceedings of the International Association for Shell and Spatial Structures (IASS) Symposium,* 2015, Amsterdam, The Netherlands.

[4] Akbarzadeh M., Van Mele T., and Block P., On the equilibrium of funicular polyhedral frames and convex polyhedral force diagrams. *Computer-Aided Design*, 2015, **63**, 118–128.

[5] Akbarzadeh M., Van Mele T., and Block P., Three-dimensional compression form finding through subdivision. In *Proceedings of the International Association for Shell and Spatial Structures (IASS) Symposium,* 2015, Amsterdam, The Netherlands.

[6] Anderson S., *Eladio Dieste: Innovation in Structural Art*. Princeton Architectural Press, New York, May 2004.

[7] Beghini L.L., Carrion J.A.B., Mazurek A., and Baker W.F., Structural optimization using graphic statics. *Structural and Multidisciplinary Optimization*, 2013, **49**, 3, 351–366.

[8] Block P., *Thrust Network Analysis: Exploring Three-dimensional Equilibrium*. PhD thesis, Massachusetts Institute of Technology, Cambridge, MA, USA, 2009.

[9] Cremona L., *Graphical Statics: Two Treatises on the Graphical Calculus and Reciprocal Figures in Graphical Statics*. Translated by Thomas Hudson Beare. Clarendon Press, Oxford, 1890.

[10] Culmann K., *Die Graphische Statik*. Verlag Meyer und Zeller, Zurich, 1864.

[11] Fivet C., and Zastavni D., Key methods from Robert Maillarts Salginatobel design process (1928). *Journal of the International Association for shell and Spatial Structures,*2012*,* **53**, 1, 39–47.

[12] Föppl A., *Das Fachwerk im Raume*. Leipzig: Verlag von B.G. Teubner, 1892.

[13] Lee J., Mueller C., and Fivet C., Automatic generation of diverse equilibrium structures through shape grammars and graphic statics. *International Journal of Space Structures,* 2016, **31**, 2-4, 146–163.

[14] Lee J., Van Mele T., and Block P., Form-finding explorations through geometric transformations and modifications of force polyhedrons. *In Proceedings of the IASS Annual Symposium 2016" Spatial Structures in the 21st Century"*, K. Kawaguchi, M. Ohsaki, and T. Takeuchi, Eds., 2016, Tokyo, Japan.

[15] Maxwell J.C., On reciprocal figures and diagrams of forces. *Philosophical Magazine Series 4, 1864,* **27**, 182, 250–261.

[16] Maxwell J.C., On reciprocal figures, frames and diagrams of forces. *Transactions of the Royal Society of Edinburgh*, 1870, **26**, 1, 1–40.

[17] McNeel R., *Rhinoceros: NURBS modeling for Windows*. Computer software, 2013.

[18] McRobie A., Maxwell and Rankine reciprocal diagrams via Minkowski sum for 2D and 3D trusses under load. *International Journal of Space Structures,*2016, **31**, 115–134.

[19] Ohlbrock P.O., D'Acunto P., Jasienski J.P., and Fivet C., Vector-Based 3D graphic statics (Part III): Designing with Combinatorial Equilibrium Modelling. *In Proceedings of the IASS Annual Symposium 2016" Spatial Structures in the 21st Century"*, K. Kawaguchi, M. Ohsaki, and T. Takeuchi, Eds., 2016, Tokyo, Japan.

[20] Preisinger C., Linking structure and parametric geometry. *Architectural Design*, 2013, **83**, 110–113.

[21] Rankine W.J.M., *A manual of applied mechanics*. Griffin, London, 1858.

[22] Rankine W.J.M., Principle of the equilibrium of polyhedral frames. *Philosophical Magazine Series 4*, 1864, **27**, 180, 92.

[23] Schek H. J., The force density method for form finding and computation of general networks. *Computer Methods in Applied Mechanics and Engineering*, 1974, **3**, 1, 115–134.

[24] Van Mele T., Lachauer L., Rippmann M., and Block P., Geometry-based understanding of structures. *Journal of the International Association for Shell and Spatial Structures*, 2012, **53**, 174, 285–295.

[25] Van Mele T., Mehrotra A., Mendez Echenagucia T., Frick U., Augustynowicz E., Ochsendorf J., DeJong M., and Block P., Form finding and structural analysis of a freeform stone vault. *In Proceedings of the International Association for Shell and Spatial Structures (IASS) Symposium 2016*, K. Kawaguchi, M. Ohsaki, and T. Takeuchi, Eds., 2016, Tokyo, Japan.

[26] Wolfe W.S., *Graphical Analysis: A Text Book on Graphic Statics*. McGraw-Hill Book Co. Inc., New York, 1921.

[27] Zastavni D., The structural design of Maillart's Chiasso shed (1924): a graphic procedure. Structural Engineering International. *The International Association for Bridge and Structural Engineering*, 2008, **18**, 3, 247–252.